**Mohamed Zellagui[1,2] *, Nasreddine Belbachir[3], Ragab A. El-Sehiemy[4] Claude Ziad El-Bayeh[5]**

J. Electrical Systems 18-1 (2022): 1-22

Journal of Electrical Systems

**Regular paper**

# Multi-Objective Optimal Allocation of Hybrid Photovoltaic Distributed Generators and Distribution Static Var Compensators in Radial Distribution Systems Using Various Optimization Algorithms

In recent years, considerable growth was about the integration of renewable energy sources in the Radial Distribution Systems (RDS), as Photovoltaic Distributed Generators (PVDG) due to their importance in achieving plenty desired technical and economic benefits. Implementation of the Distribution Static Var Compensator (DSVC) in addition to the PVDG would be one of the best choices that may provide the maximum of those benefits. Hence, it is crucial to determine the optimal allocation of the devices (PVDG and DSVC) into RDS to get satisfactory results and solutions. This paper is devoted to solve the allocation problem (locate and size) of hybrid PVDG and DSVC units into the standards test systems IEEE 33-bus and 69-bus RDSs. Solving the formulated problem of the optimal integration of hybrid PVDG and DSVC units is based on minimizing the proposed Multi-Objective Function (MOF) which is represented as the sum of the technical-economic parameters of Total Active Power Loss (TAPL), Total Reactive Power Loss (TRPL), Total Voltage Deviation (TVD), Total Operation Time (TOT) of the overcurrent relays (OCRs) installed in the RDS, the Investment Cost of PVDGs ($IC_{PVDG}$) and the Investment Cost of DSVCs ($IC_{DSVC}$), by applying various recent metaheuristic optimization algorithms. The simulation results reveal the superiority and the effectiveness of the Slime Mould Algorithm (SMA) in providing the minimum of MOF, including minimization of the power losses until 16.209 kW, and 12.11 kVar for the first RDS, 4.756 kW and 7.003 kVar for the second RDS, enhancing the voltage profiles and the overcurrent protection system. Moreover, the ability to reach the optimal allocation of PVDG and DSVC and maintain the voltage profiles in the allowable limit, whatever the load demand variation.

Keywords: photovoltaic distributed generation, distribution static var compensator, radial distribution system, optimal integration, multi-objective function, slime mould algorithm.

## 1. Introduction

The capacities of the distribution lines are usually limited. Therefore, it is necessary to consider the future load additions, and how they will be served [1]. The renewable energy sources-based Distributed Generation (DG) can help to solve the challenges mentioned above for future medium voltage Radial Distribution Systems (RDSs). Aside from traditional producing units, modern power systems incorporate a variety of Renewable Energy Sources (RESs) [2]. There are several Flexible Alternating Current Transmission System (FACTS) devices available. For now, distributed FACTS devices are the most sophisticated tools of reactive energy compensation used in RDS [3]. In RDS, the reactive power flow produces issues such as power losses, poor power factor, voltage drop, and so

* Corresponding author: M. Zellagui, Department of Electrical Engineering, University of Batna 2, Batna, Algeria, E-mail: m.zellagui@univ-batna2.dz, m.zellagui@ieee.org

[1] Department of Electrical Engineering, University of Batna 2, Batna, Algeria

[2] Department of Electrical Engineering, ETS, University of Québec, Québec, Canada

[3] Department of Electrical Engineering, University of Mostaganem, Mostaganem, Algeria

[4] Electrical Engineering Department, Faculty of Engineering, Kafrelsheikh University, Kafrelsheikh, Egypt

[5] Canada Excellence Research Chairs Team, Concordia University, Montreal, Canada

on. As a result, reactive power compensation is critical in the operation of the RDS to tackle the concerns outlined [4].

In passive RDSs, some of the achieved benefits when the Photovoltaic Distributed Generation (PVDG) sources are presented, assigned to other devices among which Distributed Static Var Compensator (DSVC) stand out. The allocation of DSVC to enhance the RDS performance is considered as one of the most affordable solutions.

For the past few years, many optimization algorithms were applied for finding the optimum allocation of PVDG and DSVC simultaneously inject both active and reactive powers in RDSs as:

- The Mixed-integer linear programming (MILP) to the maximum hosting capacity of DG and SVC in RDS in [5],
- An analytical method based the bus impedance matrix for minimizing active power loss in [6],
- Chu-Beasley Genetic Algorithm (CBGA) to reduce the investment and operation costs in [7],
- Enhanced Genetic Algorithm (EGA) to minimize both of total active power losses and the voltage deviation in [8].
- Applied fuzzy/GA technique for reducing the power supply and the active power loss in [9],
- Implemented Mutation Differential Evolution (IMDE) algorithm to mitigate the yearly cost of losses in [10],
- Adaptive Differential Search (ADS) algorithm to minimize the total power loss and total combined cost in [11].
- Particle Swarm Optimization (PSO) algorithm-based loss sensitivity factor for power loss and voltage deviation reductions in [12],
- External PSO (EPSO) algorithm to maximum value for the economic savings in [13],
- Constriction Factor PSO (CFPSO) algorithm for minimizing power losses and voltage deviation with improving the voltage stability index in [14],
- Cuckoo Search Algorithm (CSA) to reduce loss power, voltage deviation and the SVC's investment cost in [15],
- Improved Grey Wolf algorithm (IGWA) to minimize the investment costs, the active power losses, and the system voltage deviations in [16],
- Enhanced Grey Wolf Algorithm (EGWA) to minimize the investment equipment, and maximize the power losses reduction's benefits in [17],
- Biogeography-Based Optimization (BBO) algorithm for minimization of total harmonic distortion, also to reduce power losses in [18],
- Moth–Flame Optimization (MFO) algorithm applied for minimizing the voltage deviation, power losses, and the cost of annual operating in [19],
- Back-tracking Search Algorithm (BSA) for minimization the power losses in [20],
- Water Cycle Algorithm (WCA) to minimize the voltage deviation, power losses, energy cost, and emissions in [21],
- Implanted the Salp Swarm Algorithm (SSA) to attain economic, technical, and environmental benefits in [22],
- Mutated Salp Swarm Algorithm (MSSA) for the power losses minimization in [23],
- The new Gbest-guided Artificial Bee Colony (GABC) algorithm for the minimization of power losses and various costs in [24],

- An Opposition-based Competitive Swarm Optimizer (OCSO) algorithm to minimize the annual operating cost in [25].

In this paper, an allocation (location and sizing) problem of PVDG and DSVC units have been formulated in order to minimize a multi-objective function which is considered as the sum of the technical and economical parameters of total active power loss, total reactive power loss, total voltage deviation, total operation time of the overcurrent relays installed in the RDS, also the investment cost of PVDGs and DSVC devices. Solving the mentioned allocation problem of PVDGs and DSVC units was based on the application and comparing of various new optimization algorithms that been developed in the last years, which are Particle Swarm Optimization (PSO) in [26], Whale Optimizer Algorithm (WOA) in [27], Ant Lion Optimization (ALO) in [28], Grasshopper Optimization Algorithm (GOA) in [29], Salp Swarm Algorithm (SSA) in [30] and Slime Mould Algorithm (SMA) in [31]. The selected algorithms were tested on the two standards IEEE 33-bus and 69-bus radial distribution systems.

The rest of the study is composed of 4 main sections followed by a list of references, where it is organized as Section 2: presenting the models of PVDG and DSVC units. Section 3 demonstrates the evaluation of the proposed multi-objective function applied in this paper. Section 4 reveal the obtained optimal results and analysis. Section 5 contains the conclusions and the achievements including the future perspectives.

## 2. The PVDG and DSVC Modeling

### 2.1. Model of PVDG

The beta Probability Density Function (PDF) represents the model of solar irradiance of each day's hours, which is based on historical data [32]. For hourly period in the actual study, the PDF for solar irradiance was formulated in [33]:

$$f_b(s) = \begin{cases} \dfrac{\Gamma(A+B)}{\Gamma(A)\Gamma(B)} s^{(\alpha-1)}(1-s)^{(\beta-1)} & 0 \le s \le 1,\ A, B \ge 0 \\ 0 & Otherwise \end{cases} \tag{1}$$

The parameters, *B* and *A*, are defined respectively as in equations (2) and (3) as:

$$B = (1-\mu)\left(\frac{\mu(1-\mu)}{\sigma^2} - 1\right) \tag{2}$$

$$A = \frac{\mu \times B}{1-\mu} \tag{3}$$

where, $\sigma$ and $\mu$ the standard deviation and mean, respectively [34]. The solar irradiance state's probability *s* through any certain hour could be formulated as:

$$P_s\{G\} = \int_{s_1}^{s_2} f_b(s)\ ds \tag{4}$$

The PV module's output power can be formulated as in [31-35]:

$$P_{PV_0}(s) = N \times FF \times V_y \times I_y \tag{5}$$

$$FF = \frac{V_{MPP} \times I_{MPP}}{V_{oc} \times I_{sc}} \tag{6}$$

$$V_y = V_{oc} \times K_v \times T_{cy} \tag{7}$$

$$I_y = s\left[I_{sc} + K_i \times \left(T_{cy} - 25\right)\right] \tag{8}$$

$$T_{cy} = T_A + s\left(\frac{N_{OT} - 20}{0.8}\right) \tag{9}$$

where, $N$ is the modules' number, $T_A$ and $T_{cy}$ represent the ambient and cell temperatures, respectively, $K_v$ and $K_i$ are the current and voltage temperature coefficients, respectively. $N_{OT}$ illustrates the cell's nominal operating temperature, $FF$ is the fill factor, $I_{sc}$ and $V_{oc}$ represent the short-circuit current and open-circuit voltage, respectively. $I_{MPP}$ and $V_{MPP}$ represent the current and voltage at MPPT, respectively.

The total output power of the PV panel is dependent on the specification and irradiance characteristics as:

$$P_{PV}(t) = \int_{s_1}^{s_2} P_{PV_0}(s) P_s\{G\} ds \tag{10}$$

2.2. Model of DSVC

The DSVC's general circuit structure is demonstrated in Figure 1 [36], [37]. It may be seen that a DSVC is composed of a thyristor-controlled reactor shunted with a fixed capacitor.

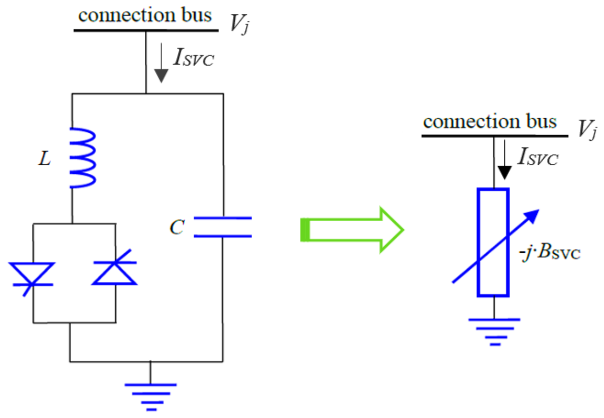


Fig. 1. A model of DSVC device: a). Circuit structure, b). Equivalent model.

The equivalent susceptance of the DSVC device ($B_{DSVC}$) is determined by the firing angle ($\alpha$) of the thyristors [36]-[38], can be expressed as follows:

$$B_{DSVC} = B_L(\alpha) + B_C \tag{11}$$

$$B_L(\alpha) = -\frac{1}{L.\omega}\left(1 - \frac{2\alpha}{\pi}\right),\ B_C = C.\omega \tag{12}$$

where, $B_C$ is the parallel capacitor reactance, $B_L$ is the series inductance reactance. $C$ and $L$ are the capacitance of the capacitor and the inductance of the reactor, respectively. $V_j$ is the value of voltage in node $j$.

The reactive power and current controlled by the DSVC device represented by the following equations:

$$Q_{DSVC} = -B_{DSVC}.V_j^2 \tag{13}$$

$$I_{DSVC} = -B_{DSVC}.V_J \tag{14}$$

When the load of the system is capacitive, the DSVC utilizes thyristor-controlled coils to consume $Q_{DSVC}$, otherwise, when the load of the system is inductive which is predominantly, the DSVC utilizes the parallel-coupled capacitors and delivers $Q_{DSVC}$, thus ameliorating voltage conditions [38]. The acceptable limits of DSVCs are also included in the formulated problem as a reactive power (inductive or capacitive) function [39], [40]:

$$-Q_{DSVC}^{\max} \le Q_{DSVC} \le +Q_{DSVC}^{\max} \tag{15}$$

where, $-Q_{DSVC}^{max}$ and $+Q_{DSVC}^{max}$ are the injected reactive power limits (inductive and capacitive operation modes) of the DSVCs, respectively.

## 3. Multi-Objective Function Evaluation

### 3.1. Multi-Objective Function

The Multi-Objective Function (*MOF*) is developed to optimally locate and size both of PVDG and DSVC units in the RDSs by minimizing simultaneously the technical and economical parameters of Total Active Power Loss (*TAPL*), Total Reactive Power Loss (*TRPL*), Total Voltage Deviation (*TVD*), Total Operation Time (*TOT*) of the overcurrent relays installed in the RDSs, the Investment Cost of PVDGs ($IC_{PVDG}$) and the Investment Cost of DSVC ($IC_{DSVC}$), where it would be formulated as follows:

$$MOF = Minimize \sum_{i=1}^{N_{Bus}} \sum_{j=2}^{N_{Bus}} \sum_{i=1}^{N_{R}} \sum_{i=1}^{N_{PVDG}} \sum_{i=1}^{N_{DSVC}} \begin{bmatrix} TAPL_{i,j} + TRPL_{i,j} + TVD_j \\ +TOT_i + IC_{PVDG,i} + IC_{DSVC,i} \end{bmatrix} \tag{16}$$

The first technical parameter is the TAPL [41], which is formulated as follows:

$$TAPL_{i,j} = \sum_{i=1}^{N_{bus}} \sum_{j=2}^{N_{bus}} APL_{i,j} \tag{17}$$

$$APL_{i,j} = \frac{R_{ij}}{V_i V_j}\cos\left(\delta_i - \delta_j\right)\left(P_i P_j + Q_i Q_j\right) + \frac{R_{ij}}{V_i V_j}\sin\left(\delta_i + \delta_j\right)\left(Q_i P_j + P_i Q_j\right) \tag{18}$$

where, $R_{ij}$ is the line resistance, and $N_{bus}$ the bus number. ($\delta_i$, $\delta_j$) and ($V_i$, $V_j$) are the angles and the voltages, respectively. ($P_i$, $P_j$) and ($Q_i$, $Q_j$) are active and reactive powers, respectively.

The second technical parameter is the TRPL [42], which is formulated as follows:

$$TRPL_{i,j} = \sum_{i=1}^{N_{bus}} \sum_{j=2}^{N_{bus}} RPL_{i,j} \tag{19}$$

$$RPL_{i,j} = \frac{X_{ij}}{V_i V_j} \cos\left(\delta_i - \delta_j\right)\left(P_i P_j + Q_i Q_j\right) + \frac{X_{ij}}{V_i V_j} \sin\left(\delta_i + \delta_j\right)\left(Q_i P_j + P_i Q_j\right) \tag{20}$$

where, $X_{ij}$ the line reactance.

The third technical parameter is the TVD [43, 44], and it is formulated as:

$$TVD_j = \sum_{j=2}^{N_{bus}} \left|1 - V_j\right| \tag{21}$$

The fourth technical parameter is the TOT of the overcurrent relay (OCR) installed in RDSs [45, 46]:

$$TOT_i = \sum_{i=1}^{N_R} T_i \tag{22}$$

$$T_i = TDS_i \left( \frac{A}{M_i^B - 1} \right) \tag{23}$$

$$M_i = \frac{I_F}{I_P} \tag{24}$$

where, $T_i$ the relay operation time, $TDS$ is the time dial setting. $A$ and $B$ are the relay constants set to 0.14, 0.02, respectively. $M$ the multiple of pickup current. $I_F$ and $I_P$ are the fault and the pickup current, respectively. $N_R$ is the number of the overcurrent relays.

The fifth economical parameter is the investment cost $IC_{PVDG}$ of PVDG [47, 48]. The $IC_{PVDG}$ as the total of installed PVDG capital cost, operation, and maintenance cost, could be formulated as:

$$IC_{PVDG} = \sum_{i=1}^{N_{PVDG}} C_{PVDG,i} . P_{PVDG,i} \tag{25}$$

where, $N_{PVDG}$, $C_{PVDG}$, and $P_{PVDG}$ are the number of PVDG units installed, the cost of one PVDG in \$/kW, and the active power injected in the distribution system by PVDG in kW, respectively. The $IC_{PVDG}$ consists of capital cost ($C_{Capital}$), operation, and maintenance ($C_{O\&M}$):

$$C_{PVDG} = C_{Capital} + C_{O\&M} \quad (\$/kW) \tag{26}$$

The capital cost is 4000 $/kW, including PV module, inverter, transportation, and installation engineering.

The final economical parameter is the investment cost $IC_{DSVC}$ of DSVC units which are placed in the system is represented by the next equation [49-52]:

$$IC_{DSVC} = \sum_{i=1}^{N_{DSVC}} C_{DSVC,i}.Q_{DSVC,i} \tag{27}$$

where, $N_{DSVC}$, $C_{DSVC}$, and $Q_{DSVC}$ the number of DSVCs installed, the cost of one DSVC in $/kVar, and the reactive power injected in RDS, respectively. The cost function of one DSVC is given by [49, 50]:

$$C_{DSVC,i} = 0.0003Q_{DSVC,i}^2 - 0.3051Q_{DSVC,i} + 127.38 \quad (\$ / kVar) \tag{28}$$

3.2. Equality Constraints

The equality constraints can be expressed by the balanced powers equations as follows:

$$P_{Sub-station} + P_{PVDG} = P_{Load} + APL \tag{29}$$

$$Q_{Sub-station} + Q_{DSVC} = Q_{Load} + RPL \tag{30}$$

where, $P_{Sub\text{-}station}$ and $Q_{Sub\text{-}station}$ are the sub-station total active and reactive powers. $P_{Load}$ and $Q_{Load}$ are the total active and reactive powers of the load demand. *APL* and *RPL* are the power losses of RDSs. $P_{PVDG}$ and $Q_{DSVC}$ are the output powers coming from PVDG and DSVC units, respectively.

3.3. Inequality Constraints

The inequality constraints for distribution system would be formulated as:

$$V_{\min} \le |V_i| \le V_{\max} \tag{31}$$

$$|1 - V_j| \le \Delta V_{\max} \tag{32}$$

$$|S_{ij}| \le S_{\max} \tag{33}$$

where, $V_{min}$ and $V_{max}$ are the minimum and maximum limits of bus voltage, $\Delta V_{max}$ is the maximum limits of voltage drop. $S_{ij}$ and $S_{max}$ are the apparent power in the distribution line and its maximum level, respectively.

3.4. PVDG and DSVC Units Constraints

The PVDG and DSVC units constraints could be formulated as follows:

$$P_{PVDG}^{\min} \le P_{PVDG} \le P_{PVDG}^{\max} \tag{34}$$

$$Q_{DSVC}^{\min} \le Q_{DSVC} \le Q_{DSVC}^{\max} \tag{35}$$

$$\sum_{i=1}^{N_{PVDG}} P_{PVDG}(i) \leq \sum_{i=1}^{N_{bus}} P_{Load}(i) \tag{36}$$

$$\sum_{i=1}^{N_{DSVC}} Q_{DSVC}(i) \leq \sum_{i=1}^{N_{bus}} Q_{Load}(i) \tag{37}$$

$$2 \leq PVDG_{Position} \leq N_{bus} \tag{38}$$

$$2 \leq DSVC_{Position} \leq N_{bus} \tag{39}$$

$$N_{PVDG} \leq N_{PVDG.\max} \tag{40}$$

$$N_{DSVC} \leq N_{DSVC.\max} \tag{41}$$

$$n_{PVDG,i} \,/\, Location \leq 1 \tag{42}$$

$$n_{DSVC,i} \,/\, Location \leq 1 \tag{43}$$

where, ($P_{PVDG}^{min}$, $Q_{DSVC}^{min}$) are the minimum of the output power injected by PVDG and DSVC, respectively. ($P_{PVDG}^{max}$, $Q_{DSVC}^{max}$) are the maximum output power injected by PVDG, and DSVC, respectively. ($N_{PVDG}$, $N_{DSVC}$) are the PVDG and DSVC units' number, respectively. ($n_{PVDG}$, $n_{DSVC}$) are the locations of PVDG and DSVC units at bus $i$, respectively.

## 4. Test Systems, Comparison and Analysis Results

### 4.1. Test systems

The performance of the competitive algorithms was examined on different standards test systems IEEE 33-bus and 69-bus RDSs [51], [52], which are represented in Figure 2. The first standard comprises total loads of 3715.00 kW and 2300.00 kVar, also with 33 buses and 32 branches. The second standard comprises total loads of 3790.00 kW and 2690.00 kVar, also with 69 buses and 68 branches. Both standards test systems operate with a nominal voltage of 12.66 kV. Each of both test systems' buses is protected by an overcurrent relay, where it would be calculated for the first system 32 relays, and 68 relays for the second system.

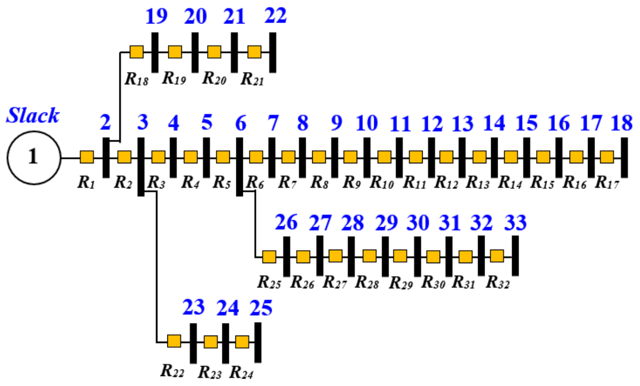


(a) IEEE 33-bus.

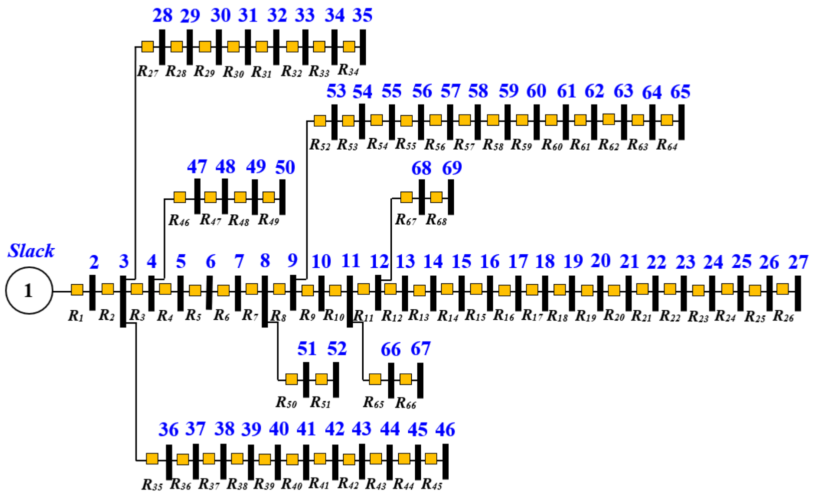


(b) IEEE 69-bus.

Fig. 2. Single diagram of test systems.

### 4.2. Comparison of Applied Algorithms

The following results were obtained for various recent algorithms on two standards test systems RDSs to minimize the MOF with a maximum iterations number of 150, and a population size equal to 10. This paper has four cases as:

Case 1: RDS without PVDG or DSVC.
Case 2: RDS with PVDG only.
Case 3: RDS with DSVC only.
Case 4: RDS with hybrid PVDG and DSVC.

Figure 3 represents the convergence curves when applying the different algorithms for the optimal hybrid PVDG and DSVC presence in both test systems RDSs.

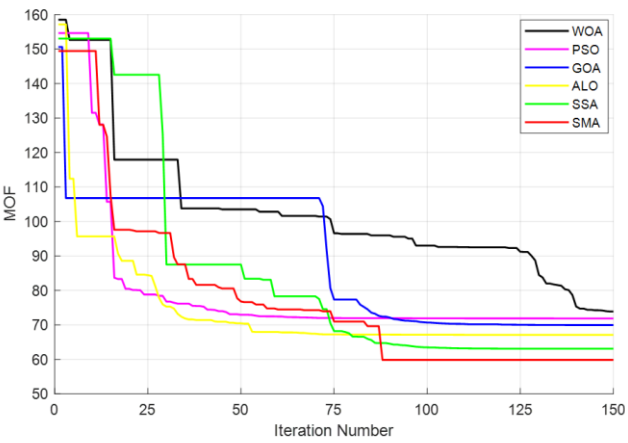


(a) IEEE 33-bus.

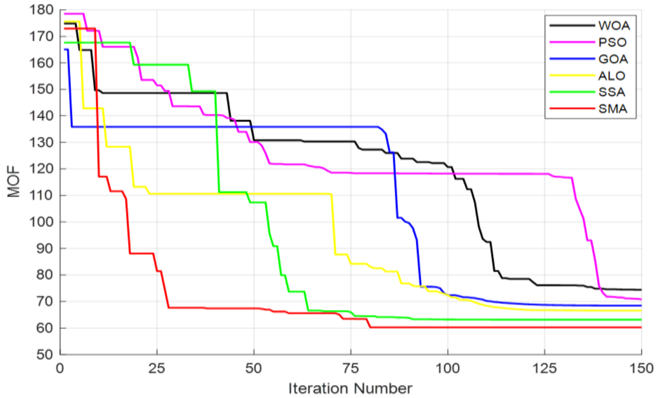


(b). IEEE 69-bus

Fig. 3. Convergence curves of algorithms for the PVDG and DSVC integration in both RDSs.

To clarify the effectiveness and robustness of the selected recent algorithms when reaching the optimal solution for the previous formulated problem, their convergence characteristics were implemented and shown in Figure 3 for both standards test systems RDSs. It may be noted after analyzing and comparing the obtained results, that all the algorithms showed good efficiency in delivering suitable results of MOF minimization.

Hence, the SMA was the best approach that provided the minimum value of the MOF for the optimal allocation of hybrid PVDG and DSVC units in both standards test systems RDSs. For the IEEE 33-bus RDS, the SMA minimized the MOF until a value of 59.828 and converges less than 90 iterations when searching for the optimal solution. For the IEEE 69-bus RDS, the SMA minimized the MOF until a value of 60.248 and converges less than 80 iterations when reaching the optimum solution.

Tables 1 and 2, contain the optimized technical and economical parameters, also the optimal allocation of hybrid PVDG and DSVC units in both standard test systems RDSs respectively, when applying the different algorithms.

In Tables 1 and 2, is revealed the effectiveness of all the applied algorithms in delivering good results for both test systems RDSs. Meanwhile, when basing on the comparison, it is obvious that the SMA was the best approach that provided the minimum MOF when optimally allocated the hybrid PVDG and DSVC units into both RDSs. Besides, the SMA showed good efficiency in delivering even the minimum of most parameters (each on its own) for both systems.

For the IEEE 33-bus RDS, the SMA minimized the TAPL until 16.209 kW and the TRPL until 12.110 kVar, with a PVDG and DSVC units' costs of 10.894 M$ and 137.027 k$, respectively. For the IEEE 69-bus RDS, the SMA technique also reduced the TAPL to 4.756 kW, the TRPL to 7.003 kVar and, the TVD until 0.134 p.u. including a medium cost of PVDG and DSVC units of 9.586 M$ and 261.854 k$, respectively.

The rest of the algorithms could not overcome the SMA in delivering the minimum MOF, nevertheless, delivered some minimum values of each parameter on their own. The ALO algorithm reduced the TVD until 0.150 p.u. and the GOA delivered the minimum PVDG units' cost of 8.074 M$ for the first standard RDS. Besides, the SSA gave the minimum PVDG units' cost of 9.387 M$ and the WOA also provided the minimum PVDG units' cost of 112.602 k$, for the second standard RDS.

Table 1: Optimal results of hybrid PVDG and DSVC for the IEEE 33-bus.

| Applied Algorithms | $P_{PVDG}$ in MW, (Bus) | $Q_{DSVC}$ in MVar, (Bus) | *TAPL* (kW) | *TRPL* (kVar) | *TVD* (p.u) | *TOT* (sec) | $TIC_{PVDG}$ (M$) | $TIC_{DSVC}$ (k$) |
|---|---|---|---|---|---|---|---|---|
| **Basic Case (Before installation)** | | | 210.987 | 143.128 | 1.812 | 20.574 | - - - | - - - |
| **WOA** | 1.0343 (10)<br>0.8385 (25)<br>0.6954 (31) | 0.0871 (3)<br>0.0951 (5)<br>1.1669 (30) | 24.431 | 18.230 | 0.418 | 20.271 | 10.324 | 228.601 |
| **PSO** | 0.8149 (6)<br>0.6736 (14)<br>0.8237 (30) | 0.8018 (7)<br>0.0748 (22)<br>0.8732 (30) | 23.704 | 18.169 | 0.233 | 20.235 | 9.295 | 147.053 |
| **GOA** | 0.5060 (11)<br>0.4344 (16)<br>1.0680 (29) | 0.3748 (13)<br>0.4119 (23)<br>1.0312 (30) | 24.158 | 17.053 | 0.185 | 20.230 | 8.074 | 178.372 |
| **ALO** | 1.2065 (6)<br>0.6355 (14)<br>0.5897 (31) | 0.4407 (12)<br>0.9312 (30)<br>0.1118 (33) | 20.941 | 15.804 | 0.150 | 20.225 | 9.775 | 129.811 |
| **SSA** | 1.0018 (11)<br>0.4926 (25)<br>0.7211 (31) | 0.4793 (12)<br>0.8119 (23)<br>0.7677 (30) | 19.590 | 13.912 | 0.282 | 20.245 | 8.906 | 140.720 |
| **SMA** | 0.9363 (11)<br>0.8616 (24)<br>0.9121 (30) | 0.4706 (12)<br>0.9618 (30)<br>0.0544 (32) | 16.209 | 12.110 | 0.194 | 20.232 | 10.894 | 137.027 |

Table 2: Optimal results of hybrid PVDG and DSVC for the IEEE 69-bus.

| Applied Algorithms | $P_{PVDG}$ in MW, (Bus) | $Q_{DSVC}$ in MVar, (Bus) | *TAPL* (kW) | *TRPL* (kVar) | *TVD* (p.u) | *TOT* (sec) | $TIC_{PVDG}$ (M$) | $TIC_{DSVC}$ (k$) |
|---|---|---|---|---|---|---|---|---|
| **Basic Case (Before installation)** | | | 224.945 | 102.139 | 1.870 | 38.772 | - - - | - - - |
| **WOA** | 0.3012 (3)<br>0.3444 (14)<br>1.7202 (61) | 0.5930 (36)<br>0.7499 (61)<br>0.5977 (62) | 14.721 | 11.064 | 0.456 | 38.543 | 9.511 | 112.602 |
| **PSO** | 0.7441 (12)<br>0.4565 (49)<br>1.7181 (61) | 1.4956 (9)<br>0.2853 (24)<br>0.9544 (61) | 12.031 | 7.610 | 0.259 | 38.500 | 11.733 | 635.001 |
| **GOA** | 0.5336 (9)<br>0.5630 (12)<br>1.5546 (63) | 0.3103 (12)<br>0.2686 (23)<br>1.1521 (61) | 9.782 | 8.990 | 0.237 | 38.517 | 10.658 | 237.800 |
| **ALO** | 0.5682 (14)<br>0.3000 (56)<br>1.5864 (62) | 0.5434 (11)<br>0.0224 (45)<br>1.2149 (61) | 9.110 | 8.591 | 0.208 | 38.501 | 9.867 | 272.503 |
| **SSA** | 0.3000 (25)<br>1.7022 (61)<br>0.3329 (68) | 0.2875 (24)<br>0.0410 (53)<br>1.1993 (61) | 6.893 | 7.903 | 0.171 | 38.511 | 9.387 | 254.802 |
| **SMA** | 0.3721 (18)<br>1.6706 (61)<br>0.3418 (66) | 0.3291 (10)<br>0.2723 (18)<br>1.1884 (61) | 4.756 | 7.003 | 0.134 | 38.507 | 9.586 | 261.854 |

Tables 3 and 4 represented a statistical analysis for the utilized algorithms which applied to optimally integrate the hybrid PVDG and DSVC units into both test systems RDSs. The statistical analysis-based on the following indices, Worst, Mean, Best, Standard Deviation (SD) and CPU Time, was carried out after 20 runs for each of the applied algorithms to prove their effectiveness and efficiency.

Based on the analysis summary, which is mentioned in Tables 3 and 4, it is clear that SMA has good efficiency in terms of all sides of the statistical analysis for both test systems RDSs, by providing the Best and the smallest Worst MOF values, also the minimum Mean and SD values, including the quickest CPU Time for its convergence characteristics when reaching the optimal solution.

Table 3. Statistical analysis of applied algorithms for the IEEE 33-bus.

| Applied Algorithms | Worst | Mean | Best | SD | CPU Time (sec) |
|---|---|---|---|---|---|
| WOA | 96.255 | 86.286 | 73.849 | 6.561 | 7.839 |
| PSO | 89.333 | 80.093 | 71.856 | 5.035 | 8.722 |
| GOA | 92.538 | 79.430 | 69.926 | 7.744 | 12.823 |
| ALO | 88.078 | 76.765 | 67.093 | 6.016 | 11.521 |
| SSA | 87.155 | 75.945 | 63.080 | 6.962 | 9.595 |
| SMA | **76.239** | **68.389** | **59.828** | **4.789** | **7.531** |

Table 4. Statistical analysis of the applied algorithms for the IEEE 69-bus.

| Applied Algorithms | Worst | Mean | Best | SD | CPU Time (sec) |
|---|---|---|---|---|---|
| WOA | 96.875 | 86.745 | 74.401 | 6.700 | 14.152 |
| PSO | 89.595 | 80.378 | 70.765 | 6.140 | 18.051 |
| GOA | 91.252 | 77.183 | 68.430 | 5.795 | 16.945 |
| ALO | 88.535 | 75.463 | 66.563 | 6.798 | 17.668 |
| SSA | 85.645 | 75.005 | 63.133 | 6.280 | 14.260 |
| SMA | **72.932** | **65.817** | **60.248** | **4.223** | **13.387** |

### 4.3. Performance of RDS Parameters

Figure 4 demonstrates the comparison of the bus voltage profiles at the basic case, and the rest of the studied cases of the optimal integration into both test systems RDSs based on the results obtained by the SMA.

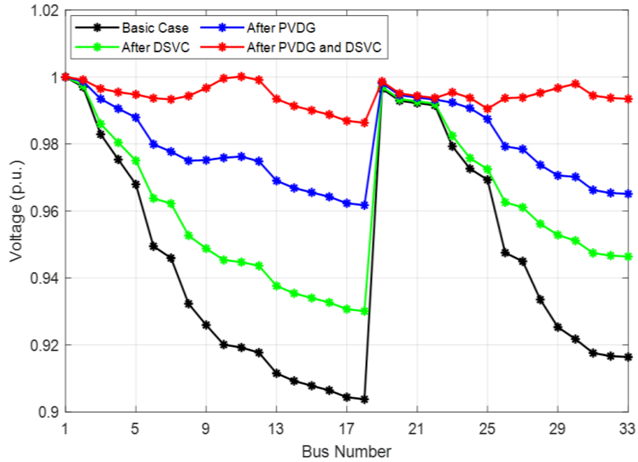


(a) IEEE 33-bus.

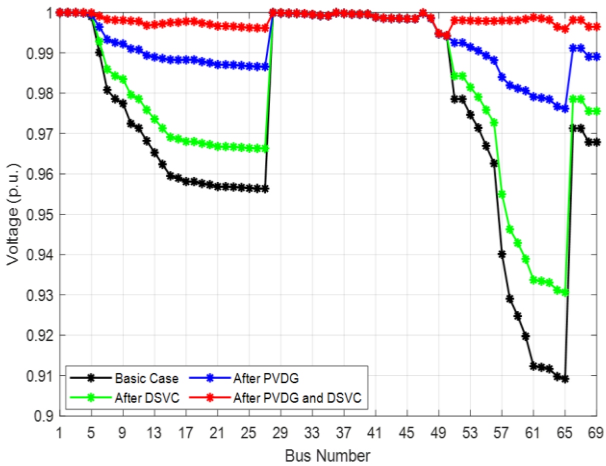


(b) IEEE 69-bus.

Fig. 4. Bus voltage profiles for RDSs.

The influence of all cases studied of the optimal integration on the voltage profiles for both test systems RDSs is mentioned in Figure 4. The voltage was improved almost in every bus of both RDSs after all cases studied integration.

Besides is noticed that superior results and a significant enhancement were achieved when integrating the case of hybrid PVDG and DSVC units into both RDSs.

This impact and enhancement were related to the minimization of voltage deviation, as long as it indicates the value of RDS's voltage and how much it is far from the nominal voltage value of 1 p.u.

Figure 5 illustrates the effect of all cases studied for the optimal integration on the active power losses variation in each branch of two test systems RDSs.

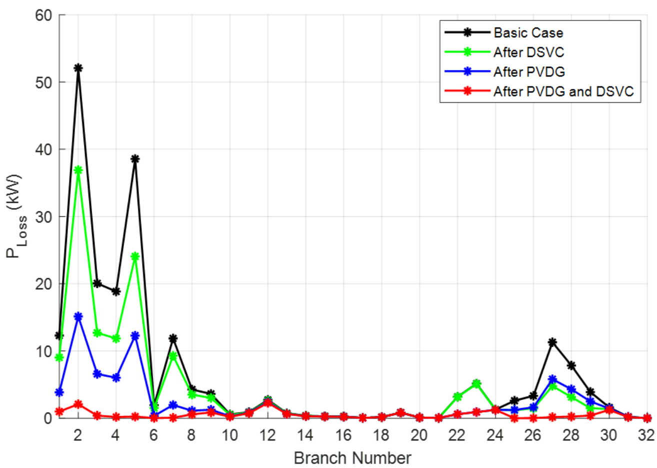


(a) IEEE 33-bus

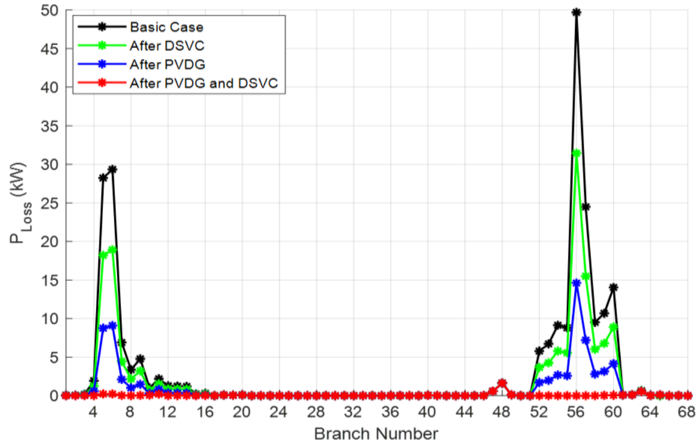


(b) IEEE 69-bus

Fig. 5. Active power losses in branches for RDSs.

Due to the structure of both the distribution systems which is radial, the active power losses are high in most of their branches, and that is why it is important to reduce them to attain many technical and economic advantages. As seen in Figure 5, the integration of all cases studied in both test systems RDSs, contributed excellently for reducing the active power losses almost in each branch of both RDSs. The case of hybrid PVDG and DSVC units provided the best results of that minimization in each branch of both RDSs if it delivers both active and reactive powers. The integration of hybrid PVDG and DSVC units also reduced the total active power losses from 210.987 kW until 16.209 kW for the IEEE 33-bus, and from 224.945 kW until 4.756 kW for the IEEE 69-bus. Figure 6 demonstrates the difference between the primary overcurrent relays' operation time at the basic case, and after the rest of the studied cases' optimal integration for both RDSs.

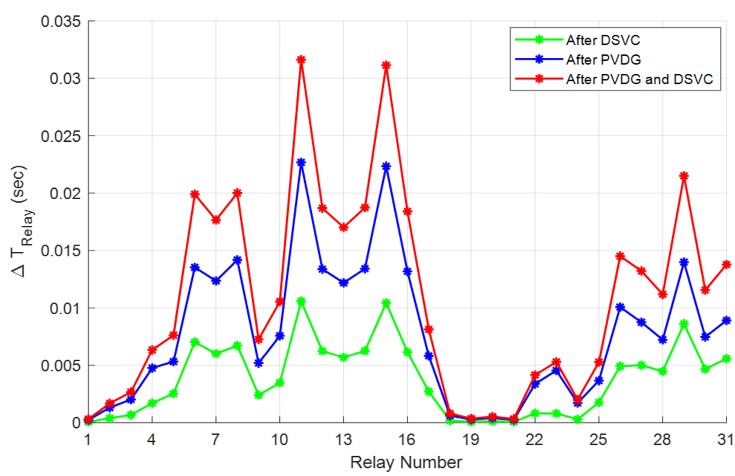


(a) IEEE 33-bus

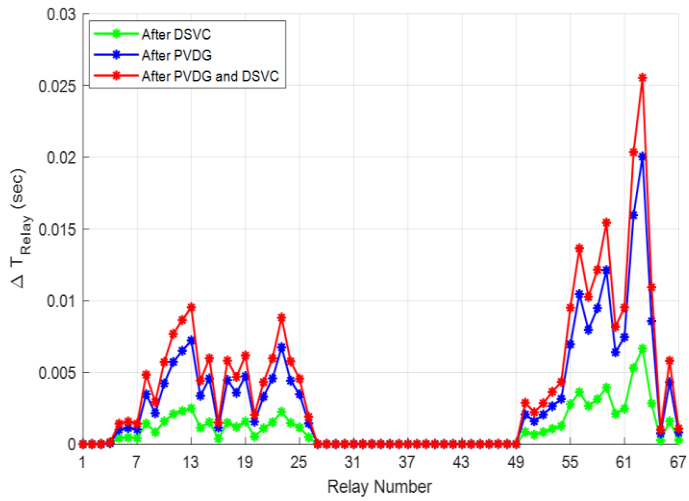


(b) IEEE 69-bus

Fig. 6. Overcurrent relay operation time for RDSs.

The main task of the overcurrent relays is to detect the fault current that occurs in the lines and do the quick isolation and protection of the system. Minimizing the operation time of those OCRs is so beneficial technically (protect the system parts) and economically (extend the equipment's lifetime).

The optimal integration of all cases studies by the SMA, led to the minimization of the operation time in all OCRs installed in both standards RDSs as illustrated in Figure 6 by $\Delta T_{Relay}$, which represents the difference between the OCR's operation time at the basic case and after the studied cases of the optimal integration into both RDSs. Also, it is clear that the hybrid PVDG and DSVC units' integration was the best case that occurs this minimization, also providing the reduction of the TOT from 20.574 seconds to 20.232 seconds for the first standard RDS, and from 38.772 seconds to 38.507 seconds for second standard RDS.

This impact was directly related to the raise of fault current which was affected by the improvement of voltage profile as mentioned in the equations (23, and 24), where the more fault current increases, the OCR will rapidly operate.

Figure 7 illustrates the graphical comparison of both total active and reactive power losses including the minimum bus voltage value after each of the optimal studied cases integration for both standards RDSs.

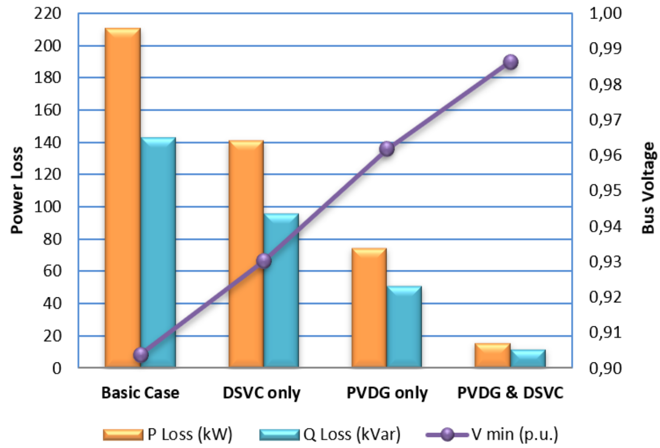


(a) IEEE 33-bus

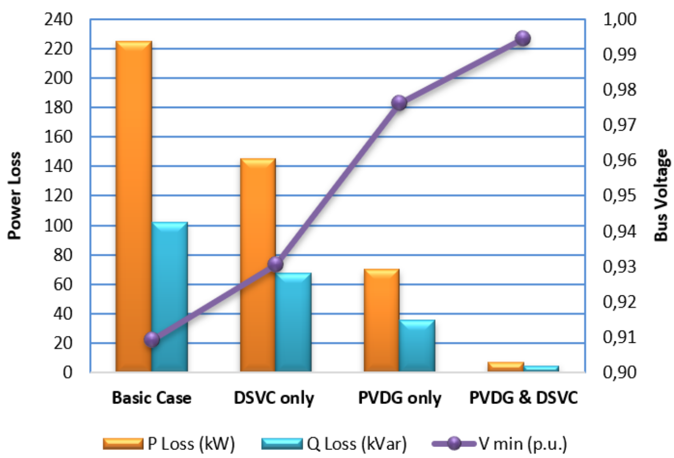


(b) IEEE 69-bus

Fig. 7. Comparison the power losses and minimum voltage.

When analyzing Figure 7, it may note that the minimum value of RDSs' voltage kept raising proportionally while the reducing of the active and reactive powers after all cases studies' optimal integration for both test systems RDSs. The best result for both terms of the minimum voltage increasing, the total power losses decreasing was provided by the case of hybrid PVDG and DSVC units' optimal integration for both standards RDSs.

The injection of both active and reactive powers by the hybrid PVDG and DSVC units into both standards RDSs reduced the active and reactive power losses until 16.209 kW and 12.110 kVar respectively, including a value of $V_{min}$ equal to 0.986 p.u. for the first RDS, meanwhile, it reduced the active and reactive power losses until 4.756 kW and 7.003 kVar respectively, including a value of the minimum voltage equal to 0.994 p.u. for the second RDS.

### 4.4. Impacts of Load Demand Variation

For the reason of validating the performance and effectiveness of the SMA approach, voltage profiles and active power losses under a different loads' variation have been implemented for both standards RDSs. For all the cases studies' optimal integration into test systems RDSs, the feeder power system loads are linearly varied from 60 % (light load) to a 120 % (peak load) with a load step of 10 %. The bus voltage profiles and the branch active power loss under various load demand variations of two RDS test systems 33-bus and 69-bus are illustrated in Figures 8 and 9, respectively.

It may note for the basic case, that the more the load is light, the voltage profiles kept improving in all buses but without reaching the optimum value (over the minimum value of 0.95 p.u.) such as in buses from 14 to 18 for the first RDS, and buses number 64 and 65 for the second RDS in Figure 8, meanwhile in Figure 9, it is seen that the active power losses in every branch were at their minimum values at the lightest load (60%) and kept raising the more the load is higher until the registration of biggest values around the peak load (120%) for both RDSs.

The optimal integration of hybrid PVDG and DSVC units, clearly enhanced the voltage profiles and significantly reduced the active power losses in every branch for both RDSs' buses comparing to the basic case. It is also clear that the more the load is light, the voltage profiles kept improving and raising, also the active power losses kept minimizing and reaching very small desirable values when the hybrid PVDG and DSVC units were optimally integrated into both RDSs.

Also, it is remarkable that even for the light and the peak loads (60% and 120%) the voltage profiles respected and stayed at the optimum range between minimum and maximum values of 0.95 p.u. and 1.05 p.u. respectively, for both test systems RDSs.

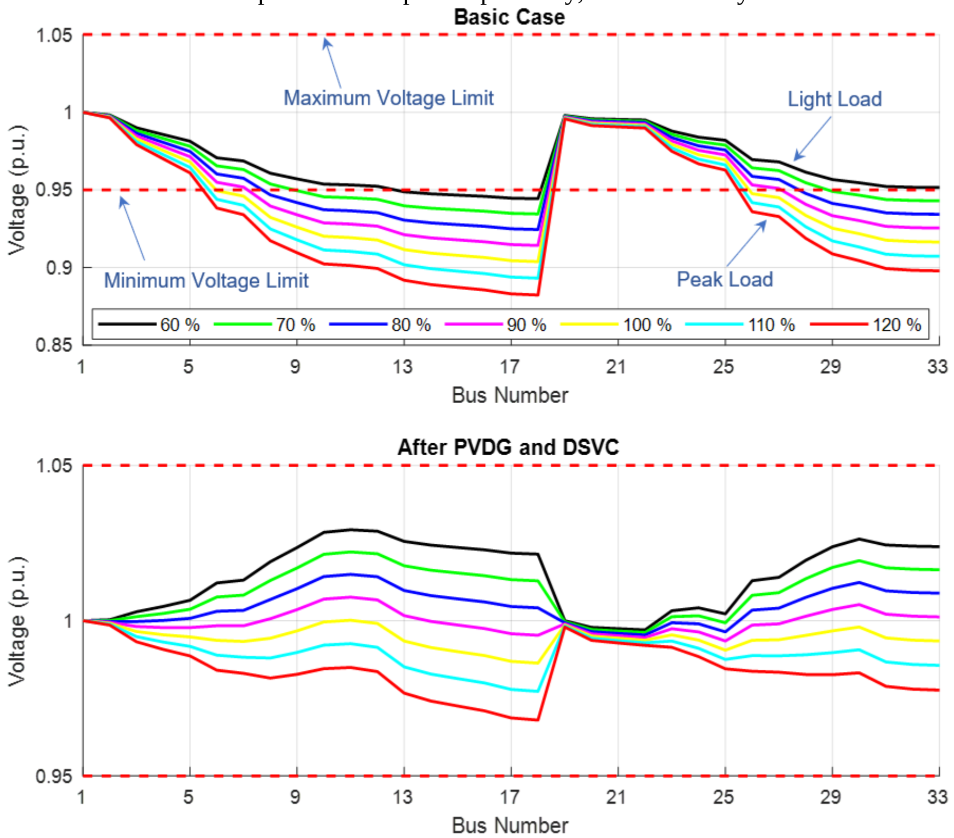


(a)

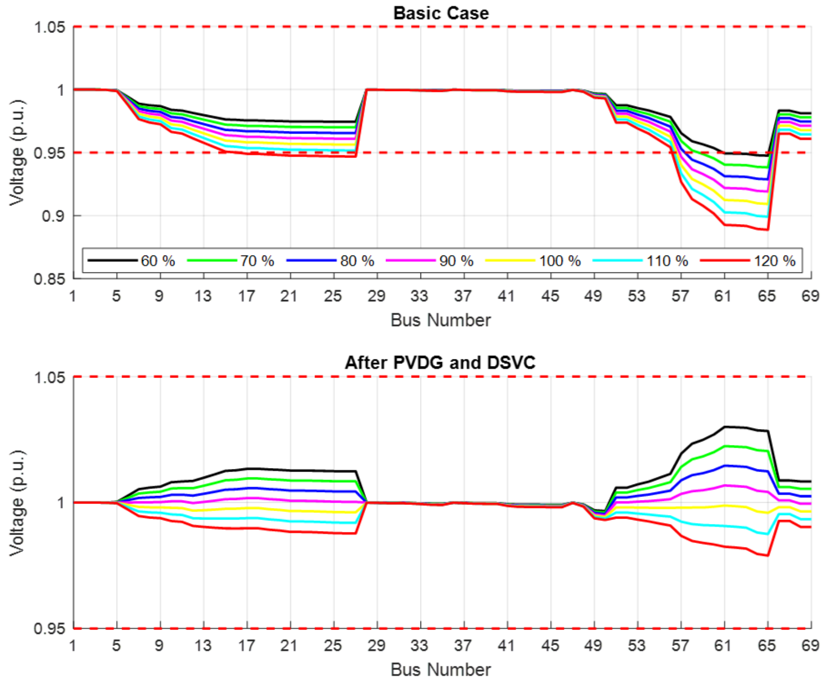


(b)

Fig. 8. Voltage profiles with various load demand variations of RDSs:
a). IEEE 33-bus, b). IEEE 69-bus.

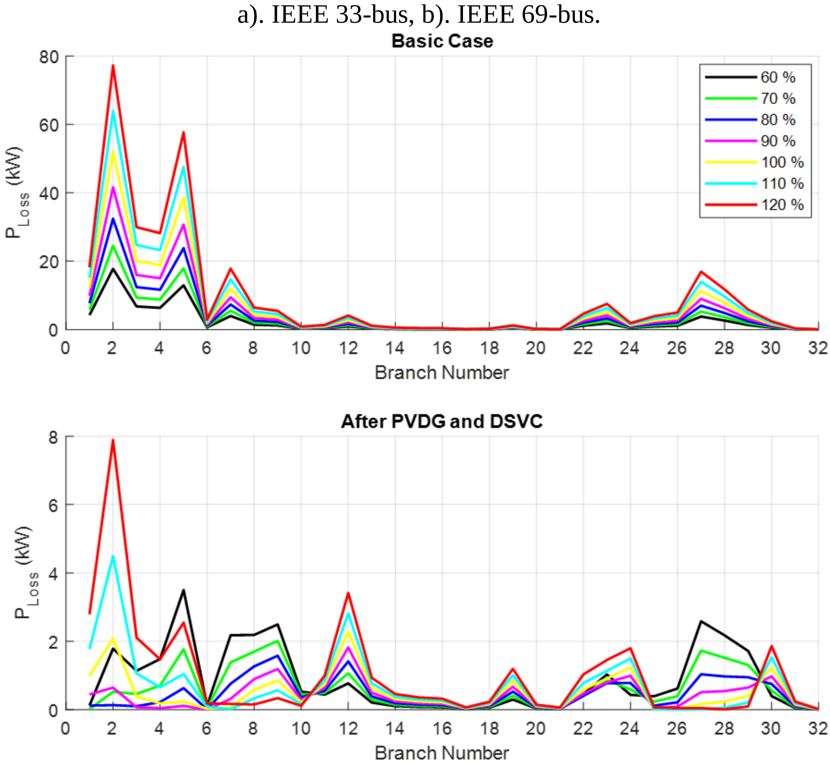


(a)

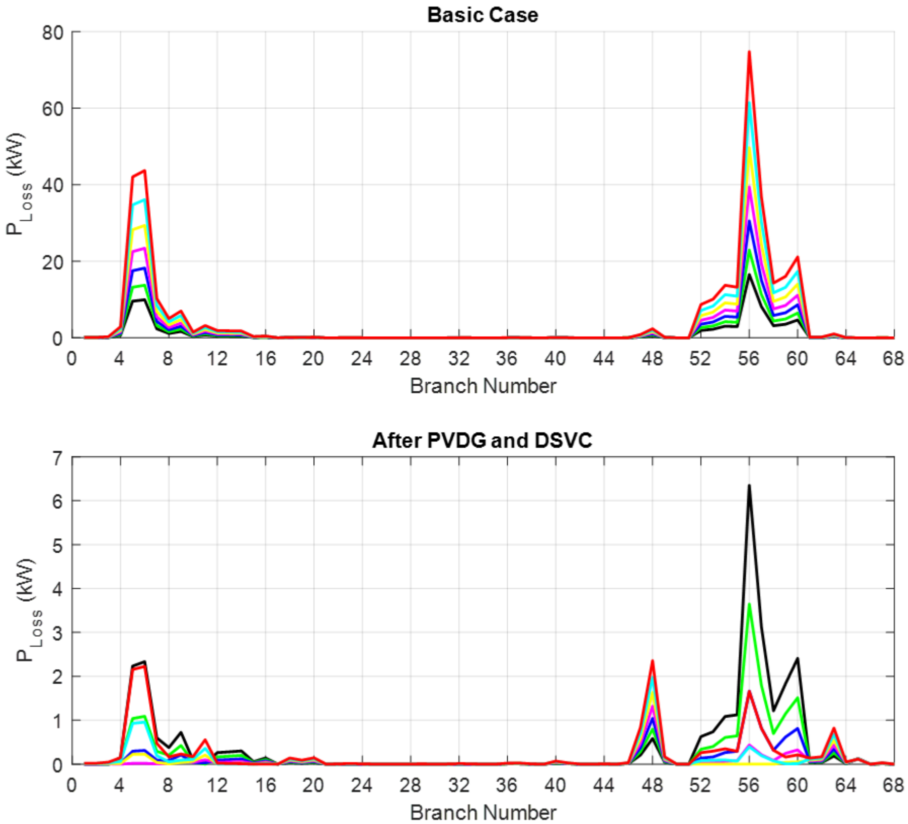


(b)

Fig. 9. Branch active power losses with different load demand variations of RDSs: a). IEEE 33-bus, b). IEEE 69-bus.

## 5. Conclusion

This paper has been compared the effectiveness and performance of recent metaheuristic optimization algorithms, which is consecrated to solve the optimal allocation problem of various studied cases into standards IEEE test systems when minimizing the multi-objective function based on technical and economic parameters.

The results reveal that the SMA technique was successfully applied and implemented to solve the mentioned formulated problem, besides, it was the best approach among the rest of the algorithms that reached the optimal solutions. The SMA showed good robustness and efficiency in delivering the best location and sizing of all cases studies with a quick convergence characteristic for both standards RDSs. The best choice that provided the best results of MOF’s minimization was the case of hybrid PVDG and DSVC units which led toward the best reducing of power losses, ameliorating voltage profiles by minimizing the voltage deviation until 0.194 p.u. for the first RDS and until 0.134 p.u. for the second RDS, enhancing the overcurrent protection system of both studied RDSs, also providing a reasonable operation and investment costs of both integrated PVDG and DSVC units all in simultaneously.

Basing the previous discussions, it is recommended to widely integrate the hybrid PVDG and DSVC units into practical RDSs. Hence, the future work will be oriented and focused on optimally allocate and implement other units as the battery energy storage systems in addition to the DSVC by applying newly optimization algorithms considering load demand uncertainties and DGs output variation, to solve a complex MOF that includes various technical-economic indices to more improvement of the studied distribution systems.

## References

[1] L. Mehigan, J. P. Deane, B. P. Ó. Gallachóir & V. Bertsch, A review of the role of distributed generation (DG) in future electricity systems. *Energy*, 163, 822–836, 2018.

[2] S. M. Ismael, S. H. A. Aleem, A. Y. Abdelaziz, & A. F. Zobaa, State-of-the-art of hosting capacity in modern power systems with distributed generation. *Renewable Energy*, 130, 002–1020, 2019.

[3] X-P. Zhang, C. Rehtanz, & B. Pal, Flexible AC transmission systems: modelling and control. Published by Springer-Verlag GmbH Germany, 2020.

[4] A. Y. Abdelaziz, E. S. Ali, & S. M. Abd Elazim, Flower pollination algorithm and loss sensitivity factors for optimal sizing and placement of capacitors in radial distribution systems. *International Journal of Electrical Power & Energy Systems*, 78, 207–214, 2019.

[5] S. Wang, S. Chen, L. Ge, & L. Wu, Distributed generation hosting capacity evaluation for distribution systems considering the robust optimal operation of OLTC and SVC. *IEEE Transactions on Sustainable Energy*, 7 (3), 1111-1123, 2016.

[6] A. Tah, & D. Das, Novel analytical method for the placement and sizing of distributed generation unit on distribution networks with and without considering P and PQV buses. *International Journal of Electrical Power & Energy Systems*, 78, 401–413, 2016.

[7] B. R. Pereira, G. R. M. da Costa, J. Contreras, & J. R. S. Mantovani, Optimal distributed generation and reactive power allocation in electrical distribution systems. *IEEE Transactions on Sustainable Energy*, 7 (3), 975–984, 2016.

[8] E. A. Almabsout, R. A. El-Sehiemy, O. N. U. An, & O. Bayat, A hybrid local search-genetic algorithm for simultaneous placement of DG units and shunt capacitors in radial distribution systems. *IEEE Access*, 8, 54465–54481, 2020.

[9] S. R. Gampa, & D. Das, Simultaneous optimal allocation and sizing of distributed generations and shunt capacitors in distribution networks using fuzzy GA methodology. *Journal of Electrical Systems and Information Technology*, 6 (4), 1–18, 2019.

[10] A. Khodabakhshian, & M. H. Andishgar, Simultaneous placement and sizing of DGs and shunt capacitors in distribution systems by using IMDE algorithm. *International Journal of Electrical Power & Energy Systems*, 82, 599–607, 2016.

[11] B. Mahdad, & K. Srairi, Adaptive differential search algorithm for optimal location of distributed generation in the presence of SVC for power loss reduction in distribution system. *Engineering Science and Technology, an International Journal*, 19 (3), 1266–1282, 2016.

[12] C. R. Kannadasan, M. H. Alsharif, M. K. Kim, & J. Nebhen, Assessment and integration of renewable energy resources installations with reactive power compensator in Indian utility power system network. *Electronics*, 10 (8), 912, 2021.

[13] M. S. Alvarez-Alvarado, C. D. Rodríguez-Gallegos, & D. Jayaweera, Optimal planning and operation of static VAR compensators in a distribution system with non-linear loads. *IET Generation, Transmission & Distribution*, 12 (15), 3726–3735, 2018.

[14] K. Balu, & V. Mukherjee, Siting and sizing of distributed generation and shunt capacitor banks in radial distribution system using constriction factor particle swarm optimization. *Electric Power Components and Systems*, 48 (7), 697–710, 2020.

[15] K. P. Nguyen, G. Fujita, & V. N. Dieu, Cuckoo search algorithm for optimal placement and sizing of static var compensator in large-scale power systems. *Journal of Artificial Intelligence and Soft Computing Research*, 6 (2), 59–68, 2016.

[16] A. A. Abou El-Ela, R. A. El-Sehiemy, A. M. Shaheen & I. A. Eissa, Optimal coordination of static VAR compensators, fixed capacitors, and distributed energy resources in Egyptian distribution networks. *International Transactions on Electrical Energy Systems*, 30 (11), e12609, 2020.

[17] A. M. Shaheen & R. A. El-Sehiemy, Optimal coordinated allocation of distributed generation units/capacitor banks/voltage regulators by EGWA. *IEEE Systems Journal*, 15 (1), 257–264, 2021.

[18] N. Ghaffarzadeh & H. Sadeghi, A new efficient BBO based method for simultaneous placement of inverter-based DG units and capacitors considering harmonic limits. *International Journal of Electrical Power & Energy Systems*, 80, 37–45, 2016.

[19] M. A. Tolba, A. A. Z. Diab, V. N. Tulsky, & A. Y. Abdelaziz, LVCI approach for optimal allocation of distributed generations and capacitor banks in distribution grids based on moth–flame optimization algorithm. *Electrical Engineering*, 100 (3), 2059–2084, 2018.

[20] W. Fadel, U. Kilic, & S. Taskin, Placement of DG, CB, and TCSC in radial distribution system for power loss minimization using back-tracking search algorithm. *Electrical Engineering*, 99 (3), 791–802, 2017.

[21] A. A. A. El-Ela, R. A. El-Sehiemy, & A. S. Abbas, Optimal placement and sizing of distributed generation and capacitor banks in distribution systems using water cycle algorithm. *IEEE Systems Journal*, 12 (4), 3629–3636, 2018.

[22] K. S. Sambaiah, & T. Jayabarathi, Optimal allocation of renewable distributed generation and capacitor banks in distribution systems using salp swarm algorithm. *International Journal of Renewable Energy Research*, 9 (1), 96–107, 2019.

[23] K. Gholami, & M. H. Parvaneh, A mutated salp swarm algorithm for optimum allocation of active and reactive power sources in radial distribution systems. *Applied Soft Computing Journal*, 85, 105833, 2019.

[24] M. Dixit, P. Kundu, & H. R. Jariwala, Incorporation of distributed generation and shunt capacitor in radial distribution system for techno-economic benefits. *Engineering Science and Technology, an International Journal*, 20 (2), 482–493, 2017.

[25] S. Das & T. Malakar, Estimating the impact of uncertainty on optimum capacitor placement in wind-integrated radial distribution system. *International Transactions on Electrical Energy Systems*, 30 (8), e12451, 2020.

[26] R. Eberhart, & J. Kennedy, A new optimizer using particle swarm theory. *6th International Symposium on Micro Machine and Human Science (MHS)*, Nagoya, Japan, 4-6 October 1995.

[27] S. Mirjalili, & A. Lewis, The whale optimization algorithm. *Advances in Engineering Software*, 95, 51–67, 2016.

[28] S. Mirjalili, The ant lion optimizer. *Advances in Engineering Software*, 83, 80–98, 2015.

[29] S. Saremi, S. Mirjalili, & A. Lewis, Grasshopper optimization algorithm: theory and application. *Advances in Engineering Software*, 105, 30–47, 2017.

[30] S. Mirjalili, A. H. Gandomi, S. Z. Mirjalili, S. Saremi, H. Faris, & S. M. Mirjalili, Salp swarm algorithm: a bio-inspired optimizer for engineering design problems. *Advances in Engineering Software*, 114, 163–191, 2017.

[31] S. Li, H. Chen, M. Wang, A. A. Heidari, S. Mirjalili, Slime mould algorithm: A new method for stochastic optimization. *Future Generation Computer Systems*, 111, 300-323, 2020.

[32] J. H. Teng, S. W. Luan, D. J. Lee, & Y. Q. Huang, Optimal charging/discharging scheduling of battery storage systems for distribution systems interconnected with sizeable PV generation systems. *IEEE Transactions on Power Systems*, 28 (2), 1425–1433, 2013.

[33] D. Q. Hung, N. Mithulananthan, & K. Y. Lee, Determining PV penetration for distribution systems with time-varying load models. *IEEE Transactions on Power Systems*, 29 (2), 3048–3057, 2014.

[34] M. Khajehvand, A. Fakharian, & M. Sedighizadeh, A hybrid approach based on IGDT-MOCMA-ES method for optimal operation of smart distribution network under severe uncertainties. *International Journal of Energy Research*, 45 (6), 9463–9491, 2021.

[35] M. Rizwan, L. Hong, W. Muhammad, S.W. Azeem, Y. Li, Hybrid harris hawks optimizer for integration of renewable energy sources considering stochastic behavior of energy sources. *International Transactions on Electrical Energy Systems*, 31 (2), e12694, 2021.

[36] S. M. Ismael, S. H. A. Aleem, A. Y. Abdelaziz, & A.F. Zobaa, State-of-the-art of hosting capacity in modern power systems with distributed generation. *Renewable Energy*, 130, 1002–1020, 2019.

[37] M. Ćalasan, T. Konjić, K. Kecojević, & L. Nikitović, Optimal allocation of static var compensators in electric power systems. *Energies*, 13, 3219, 2020.

[38] M. Zellagui, & A. Chaghi, Impact of SVC devices on distance protection setting zones in 400 kV transmission line. *UPB Scientific Bulletin, Series C: Electrical Engineering and Computer Science*, 75 (2), 249–262, 2013.

[39] A. M. Shaheen, R. A. El-Sehiemy, S. M. Farrag, A reactive power planning procedure considering iterative identification of VAR candidate buses. *Neural Computing and Applications*, 31, 653–674, 2019.

[40] E. A. Belati, C. F. Nascimento, H. de Faria, E. H. Watanabe, & A. Padilha-Feltrin, Allocation of static var compensator in electric power systems considering different load levels. *Journal of Control, Automation and Electrical Systems*, 30, 1–8, 2019.

[41] M. Zellagui, S. Settoul, A. Lasmari, C.Z. El-Bayeh, R. Chenni, & H.A. Hassan, Optimal allocation of renewable energy source integrated-smart distribution systems based on technical-economic analysis considering load demand and DG uncertainties. *Lecture Notes in Networks and Systems*, 174, 391–404, 2021.

[42] S. Settoul, R. Chenni, M. Zellagui, & H. Nouri, Optimal integration of renewable distributed generation using the whale optimization algorithm for techno-economic analysis. *Lecture Notes in Electrical Engineering*, 682, 513–532, 2021.

[43] M. Zellagui, N. Belbachir, A. Lasmari, B. Bekkouche, & C.Z. El-Bayeh, Application hybrid chaotic maps and adaptive acceleration coefficients PSO algorithm for optimal integration photovoltaic distributed

generation problem in distribution energy network. *2nd Electric Power and Renewable Energy Conference (EPREC)*, Jamshedpur, India, 28-30 May 2021.

[44] A. Lasmari, M. Zellagui, H.A. Hassan, S. Settoul, A.Y. Abdelaziz, & R. Chenni, Optimal energy-efficient integration of photovoltaic DG in radial distribution systems for various load models. *11th International Renewable Energy Congress (IREC)*, Hammamet, Tunisia, 29-31 October 2020.

[45] N. Belbachir, M. Zellagui, A. Lasmari, C.Z. El-Bayeh, & B. Bekkouche, Optimal PV sources integration in distribution system and its impacts on overcurrent relay based time-current-voltage tripping characteristic. *12th International Symposium on Advanced Topics in Electrical Engineering (ATEE)*, Bucharest, Romania, 25-27 March 2021.

[46] H. R. E. H. Bouchekara, M. Zellagui, & M. A. Abido, Optimal coordination of directional overcurrent relays using a modified electromagnetic field optimization algorithm. *Applied Soft Computing Journal*, 54, 267–283, 2017.

[47] E. Grover-Silva, R. Girard, & G. Kariniotakis, Optimal sizing and placement of distribution grid connected battery systems through an SOCP optimal power flow algorithm. *Applied Energy*, 219, 385–393, 2018.

[48] K. E. Adetunji, I. W. Hofsajer, A. M. Abu-Mahfouz, & L. Cheng, A review of Metaheuristic techniques for optimal integration of electrical units in distribution networks. *IEEE Access*, 9, 5046–5068, 2021.

[49] M. Nadeem, K. Imran, A. Khattak, A. U. Pal, A. M. Z. Zeb, A. N. Khan, & M. Padhee, Optimal placement, sizing, and coordination of FACTS devices in transmission network using whale optimization algorithm. *Energies*, 13(3), 753, 2020.

[50] X. Xu, J. Li, Z. Xu, J. Zhao, & C. S. Lai, Enhancing photovoltaic hosting capacity – A stochastic approach to optimal planning of static var compensator devices in distribution networks. *Applied Energy*, 238, 952–962, 2019.

[51] A. M. Shaheen, A. M. Elsayed, R. A. El-Sehiemy, S. Kamel, & S. S. Ghoneim, A modified marine predators optimization algorithm for simultaneous network reconfiguration and distributed generator allocation in distribution systems under different loading conditions. *Engineering Optimization*, 54 (3), 1–22, 2021.

[52] M. Zellagui, A. Lasmari, S. Settoul, R. A. El- Sehiemy, C. Z. El- Bayeh, & R. Chenni, Simultaneous allocation of photovoltaic DG and DSTATCOM for techno- economic and environmental benefits in electrical distribution systems at different loading conditions using novel hybrid optimization algorithms. *International Transactions on Electrical Energy Systems*, 31 (8), e12992, 2021.